observed trends in the photochemical quantum yields; however, our results do suggest a correlation between σ-donor abilities of the ligands, L, and the photoaquation quantum yields. (3) The luminescence spectra of the complexes are sensitive to the nature of the unique ligand, and a definite correlation between the emission band maximum and the photoaquation quantum yield exists: as the energy of the emission band maximum decreases, the photochemical quantum yield increases. (4) Increases in Φ_L at 298 K are paralleled by increases in the radiationless deactivation rate constants at 77 K as L is varied, thus indicating a close connection between the structural factors which affect photochemical and photophysical radiationless decay processes in these complexes.

Acknowledgments. This work was supported by the National Science Foundation (GP-26199 and GP-36643X). The rhodium used in these studies was provided on loan by Matthey-Bishop, Inc.

References and Notes

(1) (a) Taken from the Ph.D. Dissertation of J.D.P., University of California, Santa Barbara, 1975. (b) Reported in part at the 165th National Meeting of the American Chemical Society, Dallas, Texas, April 1973, INORG 39; and at the 169th National Meeting of the American Chemical Society, Philadelphia, Pa., April 1975, INORG 141.
(2) Camille and Henry Dreyfus Foundation Teacher–Scholar, 1971–1976.
(3) General reviews are: (a) V. Balzani and V. Carassiti, "Photochemistry of Coordination Compounds", Academic Press, London, 1970; (b) P. D. Fleischauer, A. W. Adamson, and G. Satori, *Prog. Inorg. Chem.*, **17**, 1 (1972); (c) A. W. Adamson and P. D. Fleischauer, Ed., "Concepts of Inorganic Photochemistry", Wiley, New York, N.Y., 1975.
(4) P. C. Ford, J. D. Petersen, and R. E. Hintze, *Coord. Chem. Rev.*, **14**, 67 (1974).
(5) R. A. Pribush, C. K. Poon, C. M. Bruce, and A. W. Adamson, *J. Am. Chem. Soc.*, **96**, 3027 (1974).
(6) (a) T. L. Kelly and J. F. Endicott, *J. Phys. Chem.*, **76**, 1937 (1972); (b) L. Moggi, *Gazz. Chim. Ital.*, **97**, 1089 (1967).
(7) T. R. Thomas and G. A. Crosby, *J. Mol. Spectrosc.*, **38**, 118 (1971).
(8) T. R. Thomas, R. J. Watts, and G. A. Crosby, *J. Chem. Phys.*, **59**, 2123 (1973).
(9) J. E. Hillis and M. K. DeArmond, *J. Lumin.*, **4**, 273 (1971).
(10) T. L. Kelly and J. F. Endicott, *J. Am. Chem. Soc.*, **94**, 1797 (1972).
(11) (a) J. L. Reed, H. D. Gafney, and F. Basolo, *J. Am. Chem. Soc.*, **96**, 1363 (1974); (b) G. Ferraudi and J. F. Endicott, *ibid.*, **95**, 2371 (1973).
(12) P. C. Ford and J. D. Petersen, *Inorg. Chem.*, **14**, 1404 (1975).
(13) J. D. Petersen and P. C. Ford, *J. Phys. Chem.*, **78**, 1144 (1974).
(14) C. Kutal and A. W. Adamson, *Inorg. Chem.*, **12**, 1454 (1973).
(15) M. M. Muir and W. L. Huang, *Inorg. Chem.*, **12**, 1831 (1973).
(16) R. D. Foust and P. C. Ford, *Inorg. Chem.*, **11**, 899 (1972).
(17) C. Cruetz and H. Taube, *J. Am. Chem. Soc.*, **95**, 1086 (1973).
(18) D. A. Chalsson, R. E. Hintze, D. H. Stuermer, J. D. Petersen, D. P. McDonald, and P. C. Ford, *J. Am. Chem. Soc.*, **94**, 6665 (1972).
(19) J. Joussot-Dublen and J. Houdard, *Tetrahedron Lett.*, **44**, 4389 (1967).
(20) G. L. Geoffroy, M. S. Wrighton, G. S. Hammond, and H. B. Gray, *Inorg. Chem.*, **13**, 430 (1974).
(21) D. A. Buckingham, F. R. Keene, and A. M. Sargeson, *J. Am. Chem. Soc.*, **95**, 5649 (1973).
(22) Given the magnitude of spin–orbit coupling for rhodium(III), the term "triplet" may have questionable validity. However, the observation of sensitization by triplet donors and energy differences between lower energy absorption bands and the emission bands point to the presence of LF states of a character in most respects analogous to the triplet proposed for compounds of the lighter elements. Therefore with some reservation we will conform to the previous description (see ref 4, 6–8, 13, 20) of such states as "triplets".
(23) D. H. Carstens and G. A. Crosby, *J. Mol. Spectrosc.*, **34**, 113 (1970).
(24) R. D. Foust and P. C. Ford, *J. Am. Chem. Soc.*, **94**, 5686 (1972).
(25) R. J. Allen and P. C. Ford, *Inorg. Chem.*, **11**, 679 (1972).
(26) M. J. Incorvia and J. I. Zink, *Inorg. Chem.*, **13**, 2489 (1974).
(27) R. Englman and J. Jortner, *Mol. Phys.*, **18**, 145 (1970).
(28) W. M. Gelbart, K. F. Freed, and S. A. Rice, *J. Chem. Phys.*, **52**, 2460 (1970).
(29) E. W. Schlag, S. Schneider, and S. F. Fischer, *Annu. Rev. Phys. Chem.*, **22**, 465 (1971).
(30) D. J. Robbins and A. J. Thompson, *Mol. Phys.*, **25**, 1103 (1973).
(31) M. Wrighton, H. B. Gray, and G. S. Hammond, *Mol. Photochem.*, **5**, 165 (1973).
(32) J. F. Endicott, presented at the VIIIth International Conference of Photochemistry, Edmonton, Alberta, Canada, Aug 1975.
(33) F. Monocelli and E. Viel, *Inorg. Chim. Acta*, **1**, 467 (1967).

The Temperature Dependence of the Crystal and Molecular Structure of $\Delta^{2,2'}$-Bi-1,3-dithiole [TTF] 7,7,8,8-Tetracyano-*p*-quinodimethane [TCNQ]

Arthur J. Schultz,[1a] Galen D. Stucky,* [1a] Robert H. Blessing,[1b] and Philip Coppens[1b]

Contribution from the Department of Chemistry and the Materials Research Laboratory, University of Illinois, Urbana, Illinois 61801, and the Department of Chemistry, State University of New York at Buffalo, Buffalo, New York 14214. *Received June 17, 1975*

Abstract: In order to structurally define the 53 K metal-insulator transition observed in the charge transfer salt, $\Delta^{2,2'}$-bi-1,3-dithiole [TTF] 7,7,8,8-tetracyano-*p*-quinodimethane [TCNQ], the structures of (TTF) (TCNQ) were examined at 60, 53, and 45 K by single-crystal x-ray diffraction. Systematic changes in other properties of the crystalline complex do appear to be related to the metal-insulator transition temperature. The minimum interplanar spacings along the homologous chains are found to be 3.408 (2) and 3.090 (1) Å for TTF and TCNQ, respectively.

The metal-insulator transition in the one-dimensional conductor TTF-TCNQ has been a subject of intensive investigation following its initial report.[2] The transition is characterized by a conductivity maximum at ~58 K now believed to be on the order of 10–30 times the room temperature conductivity.[3] It was proposed[2b] that a possible mechanism for this behavior would involve a soft phonon mode producing paraconductivity as a result of a lattice distortion at the transition temperature. This type of lattice distortion associated with the metal to insulator transition in one-dimensional conductors is believed to occur in the Krogmann salts, $[K_2Pt(CN)_4]X_{0.3}\cdot XH_2O$ (X = Cl, Br), where evidence for a soft phonon mode, through the observation of a Kohn anomaly, has been reported.[4,5] However, the Krogmann salts do not exhibit a sharp rise and fall in conductivity, and it is this property in TTF-TCNQ that has generated much interest.

The single-crystal x-ray diffraction structures of TTF-TCNQ previously have been reported for room temperature[6] and 100 K[7] data. In this paper, we present the structural results for data collected at 60 K, where the transition, as defined by the heat capacity data, is beginning; at 53 K, where the maximum peak in the heat capacity curve occurs;[8] and at 45 K, which is well into the insulating state. Simi-

Table I. Data Collection and Refinement

	60 K	53 K	45 K
Crystal size,[a] mm	0.59 × 0.19 × 0.11		0.50 × 0.05 × 0.005
Total no. of independent refls measd	2314	2397	1551
No. of refls with $I > 2\sigma(I)$	1397	1445	
Final R factor	0.071[b]	0.084[b]	0.042[c] 0.058[d]
Final R_w factor	0.058[b]	0.077[b]	0.052[c] 0.092[d]

[a] Dimensions correspond to the b, a, and c^* directions, respectively. [b] Refinement on F_o with $I > 2\sigma(I)$. [c] Refinement on F_o with all reflections (including $F_o^2 = 0$). [d] Refinement on F_o^2 with all reflections (including $F_o^2 = 0$).

lar experimental studies relevant to the second transition noted earlier at 38 K[9] are in progress and will be reported in a subsequent publication.

Experimental Section

The crystals used in this study were grown by codiffusion of TTF and TCNQ in acetonitrile at Buffalo, Illinois, and Monsanto Laboratories. A large number of specimens were examined because of the tendency of the complex to form twinned or poorly formed crystals. The crystal finally selected for data collection at 53 and 60 K had been used for conductivity measurements at Monsanto Laboratories and unlike many specimens which were examined exhibited a value of $\sigma(58)/\sigma(RT)$ of ~20. It was found that cycling of this sample and the 45 K sample through the transition temperature did not result in any noticeable degradation of the diffraction intensities. Weissenberg and precession photographs were in agreement with the previously reported[6] space group of $P2_1/c$ of the monoclinic class with two molecules of TTF-TCNQ per unit cell.

The crystals were mounted in thin-walled glass capillaries along the b-axis direction. The crystal dimensions are given in Table I along with other information pertaining to data collection and refinement. Low temperature data were collected on Picker FACS-I diffractometers equipped with a Cryogenics Associates CT-38 cryostat.[10] The cell dimensions obtained at 40 K were used in refinement of the 45 K structure, since no significant differences were observed at the two temperatures. The values used for final refinement of the 53 and 60 K data were obtained from the powder diffraction results shown in Figure 1[11] and do not differ from the measured single crystal values at 53 and 60 K by more than one standard deviation. Data were collected using zirconium-filtered Mo Kα radiation (λ 0.71069 Å). Reflections with 2θ values between 5 and 55 K were measured and corrected for Lorentz and polarization effects and the absorption of the beryllium shrouds of the cryostat to yield a set of F_o values where F_o is the observed structure factor amplitude.

The initial positional parameters used for refinement were those reported for the room temperature structure of TTF-TCNQ.[6] The function minimized in the 53 and 60 K least-squares refinements

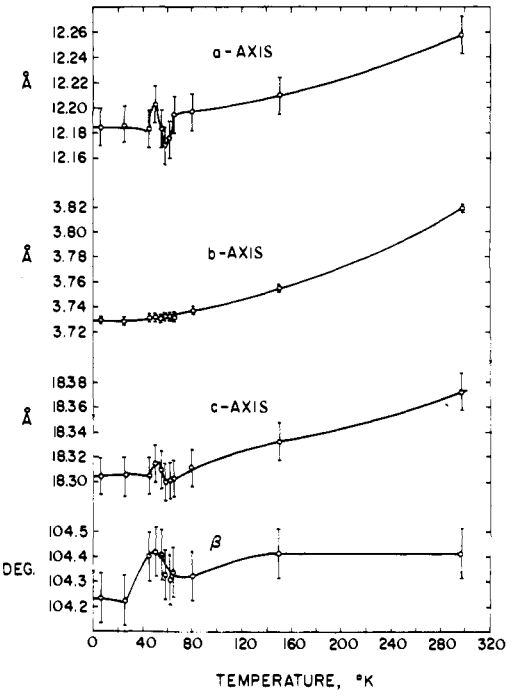

Figure 1. Cell parameters plotted against temperature.

was $\Sigma w(|F_o| - |F_c|)^2$ where the weights w were assigned as $2F_o/\sigma(F_o^2)$. The standard deviations $\sigma(F_o^2)$ were estimated according to the formula

$$\sigma(F_o^2) = (\mathrm{Lp})^{-1}[S + (B_1 + B_2)(T_S/2T_B)^2 + (0.03I)^2]^{1/2}$$

where S, B_1, and B_2 are the scan and background counts in times T_S and T_B, Lp is the Lorentz-polarization factor, and I is the integrated intensity. For the 45 K structure, the function minimized was $\Sigma w(F_o^2 - |F_c|^2)^2$ with weights w of $1/\sigma^2(F_o^2)$ where $\sigma(F_o^2)$ was the larger of the above calculation or a calculation based on the observed variances of symmetry equivalent reflections. The 45 K refinement included an isotropic extinction parameter, but absorption was ignored for all three studies (μ = 5.6 cm^{-1}). The effect of anomalous scattering was included for the sulfur atoms, and all nonhydrogen atoms were assigned anisotropic thermal parameters. The final discrepancy indices R and R_w are given in Table I. The final parameters for the structure at each temperature are given in Table III along with their standard deviations as obtained from the inverse matrix. A table of the F_o and F_c values for the reflections used in the final refinements is available.[12]

Description of the Structure and Discussion

As has been described elsewhere,[6,7] the crystal structure consists of discreet linear chains of TTF and TCNQ stacking parallel to the b axis (Figure 2) with both TTF and TCNQ molecules situated on crystallographic centers of inversion. The labeling scheme and thermal ellipsoids for TTF and TCNQ at 53 K are shown in Figures 3 and 4, respectively. Table IV provides the intramolecular bond dis-

Table II. Crystal Data for (TTF)(TCNQ)

$C_{18}H_8N_4S_4$ M = 408.5 D
Monoclinic (b-axis unique)
$P2_1/c$

	40 K[a]	53 K[b]	60 K[b]	100 K[a]	295 K[a]
a (Å)	12.210 (5)	12.191 (10)	12.173 (10)	12.228 (6)	12.302 (6)
b (Å)	3.729 (1)	3.731 (2)	3.733 (2)	3.754 (1)	3.817 (1)
c (Å)	18.343 (6)	18.312 (10)	18.301 (10)	18.379 (10)	18.449 (9)
β (deg)	104.38 (2)	104.43 (2)	104.33 (2)	104.42 (4)	104.49 (5)
V (Å^3)	809.0 (5)	806.6 (8)	805.8 (8)	817.0 (7)	838.7 (3)
ρ(calcd)(g/cm^3)	1.68	1.68	1.68	1.66	1.62

[a] The unit cell dimensions were determined from a least-squares refinement of the angular settings of 26 diffractometer-centered reflections of a single crystal (ref 7). [b] The cell dimensions were obtained from powder data measured by G. A. Jones, Central Research Department, du Pont (private communication from L. J. Guggenberger).

Table III. Final Positional and Thermal Parameters for TTF–TCNQ at 45, 53, and 60 K

Atom	x^a	y	z	U (Å^2)^b
S(1)	−0.09416 (4)	−0.1843 (1)	0.07987 (3)	c
	−0.0941 (1)	−0.1836 (5)	0.07986 (8)	c
	−0.09389 (9)	−0.1841 (4)	0.07988 (6)	c
S(2)	0.14864 (4)	−0.1807 (1)	0.08545 (3)	c
	0.1485 (1)	−0.1811 (5)	0.08548 (8)	c
	0.14832 (9)	−0.1806 (4)	0.08531 (6)	c
N(1)	0.3837 (1)	0.6053 (5)	0.1908 (1)	c
	0.3836 (5)	0.6054 (13)	0.1909 (3)	c
	0.3840 (3)	0.6054 (10)	0.1906 (2)	c
N(2)	0.7508 (1)	0.6347 (5)	0.1903 (1)	c
	0.7507 (4)	0.6342 (13)	0.1902 (3)	c
	0.7503 (3)	0.6332 (10)	0.1901 (2)	c
C(1)	−0.0019 (2)	−0.3399 (5)	0.1612 (1)	c
	−0.0006 (5)	−0.3424 (18)	0.1610 (3)	c
	−0.0012 (4)	−0.3401 (14)	0.1610 (2)	c
C(2)	0.1094 (2)	−0.3393 (5)	0.1640 (1)	c
	0.1079 (5)	−0.3374 (18)	0.1637 (3)	c
	0.1076 (4)	−0.3395 (14)	0.1635 (3)	c
C(3)	0.0116 (1)	−0.0779 (5)	0.0349 (1)	c
	0.0121 (5)	−0.0760 (16)	0.0343 (3)	c
	0.0113 (3)	−0.0766 (12)	0.0344 (2)	c
C(4)	0.4582 (1)	0.5233 (5)	0.1665 (1)	c
	0.4579 (5)	0.5189 (17)	0.1665 (3)	c
	0.4582 (4)	0.5235 (13)	0.1661 (2)	c
C(5)	0.6588 (1)	0.5374 (5)	0.1663 (1)	c
	0.6600 (5)	0.5369 (16)	0.1659 (3)	c
	0.6597 (4)	0.5378 (12)	0.1665 (2)	c
C(6)	0.5470 (1)	0.4191 (5)	0.1323 (1)	c
	0.5471 (5)	0.4193 (16)	0.1327 (3)	c
	0.5474 (4)	0.4175 (12)	0.1323 (2)	c
C(7)	0.5239 (1)	0.2095 (5)	0.0674 (1)	c
	0.5234 (5)	0.2085 (16)	0.0677 (3)	c
	0.5237 (3)	0.2109 (12)	0.0676 (2)	c
C(8)	0.4105 (1)	0.0945 (5)	0.0313 (1)	c
	0.4106 (5)	0.0938 (16)	0.0315 (3)	c
	0.4109 (4)	0.0929 (12)	0.0315 (3)	c
C(9)	0.6116 (1)	0.1053 (5)	0.0316 (1)	c
	0.6102 (5)	0.1070 (15)	0.0320 (4)	c
	0.6110 (4)	0.1045 (12)	0.0319 (3)	c
H(1)	−0.031 (2)	−0.434 (6)	0.203 (1)	0.013 (6)
	−0.033 (5)	−0.408 (19)	0.190 (3)	0.013^d
	−0.037 (4)	−0.433 (13)	0.199 (2)	0.013
H(2)	0.171 (2)	−0.435 (6)	0.208 (1)	0.005 (5)
	0.163 (5)	−0.419 (17)	0.206 (3)	0.013
	0.161 (4)	−0.418 (13)	0.202 (2)	0.013
H(8)	0.357 (2)	0.167 (6)	0.057 (1)	0.012 (6)
	0.350 (5)	0.171 (17)	0.062 (3)	0.013
	0.356 (4)	0.169 (13)	0.052 (2)	0.013
H(9)	0.681 (2)	0.192 (6)	0.054 (1)	0.011 (6)
	0.685 (5)	0.217 (16)	0.060 (3)	0.013
	0.680 (4)	0.173 (13)	0.051 (2)	0.013

	Anisotropic Thermal Parameters (×10^4)^e					
Atom	U_{11}	U_{22}	U_{33}	U_{12}	U_{13}	U_{23}
S(1)	51 (3)	85 (3)	84 (3)	3 (2)	32 (2)	10 (2)
	83 (7)	113 (7)	165 (8)	2 (7)	−15 (6)	16 (7)
	104 (6)	136 (5)	171 (6)	2 (6)	43 (4)	14 (6)
S(2)	44 (2)	87 (3)	75 (3)	6 (2)	17 (2)	11 (2)
	82 (7)	116 (7)	170 (8)	−6 (7)	−40 (6)	23 (7)
	97 (5)	137 (6)	171 (6)	11 (6)	29 (4)	20 (6)
N(1)	97 (8)	112 (9)	91 (10)	−4 (6)	22 (7)	−10 (8)
	157 (28)	105 (27)	236 (30)	18 (23)	−18 (24)	−20 (23)
	184 (20)	157 (22)	211 (22)	12 (18)	41 (17)	−25 (18)
N(2)	100 (8)	113 (9)	129 (10)	4 (6)	52 (8)	2 (8)
	142 (27)	125 (28)	251 (30)	13 (24)	22 (23)	19 (24)
	149 (19)	142 (21)	164 (20)	16 (18)	35 (16)	10 (18)
C(1)	83 (8)	89 (10)	43 (11)	2 (7)	8 (8)	15 (8)
	159 (32)	135 (29)	159 (32)	−15 (31)	−30 (26)	18 (30)
	193 (24)	149 (22)	130 (23)	−3 (24)	10 (19)	−9 (23)
C(2)	102 (9)	67 (10)	74 (11)	−3 (7)	31 (9)	4 (8)
	145 (32)	137 (29)	191 (32)	−42 (31)	−75 (26)	9 (30)
	154 (23)	137 (22)	157 (23)	0 (23)	−3 (18)	28 (23)
C(3)	46 (8)	73 (9)	115 (11)	−2 (7)	37 (8)	−14 (9)
	50 (27)	78 (25)	282 (35)	−11 (24)	−19 (26)	4 (26)
	31 (18)	122 (20)	137 (21)	−9 (18)	10 (17)	4 (18)

Table III. *Continued*

Atom	U_{11}	U_{22}	U_{33}	U_{12}	U_{13}	U_{23}
C(4)	86 (8)	45 (9)	23 (10)	−22 (7)	−21 (8)	−11 (8)
	138 (34)	52 (28)	145 (32)	7 (26)	−108 (27)	26 (24)
	110 (23)	105 (23)	137 (24)	26 (19)	−72 (19)	−8 (19)
C(5)	118 (9)	51 (9)	50 (10)	19 (7)	44 (8)	2 (8)
	108 (31)	66 (26)	179 (33)	50 (26)	−21 (26)	−29 (26)
	144 (23)	96 (21)	151 (24)	25 (20)	40 (19)	13 (20)
C(6)	76 (8)	52 (9)	69 (11)	14 (7)	29 (8)	27 (9)
	114 (30)	118 (28)	178 (33)	20 (26)	−65 (26)	10 (27)
	128 (21)	102 (21)	152 (23)	25 (19)	29 (18)	−4 (19)
C(7)	69 (9)	38 (9)	71 (11)	19 (7)	22 (8)	39 (8)
	76 (26)	61 (23)	182 (32)	40 (26)	25 (24)	36 (25)
	115 (20)	92 (19)	161 (24)	53 (20)	37 (18)	69 (20)
C(8)	64 (8)	59 (9)	95 (11)	16 (7)	45 (8)	19 (8)
	114 (30)	109 (28)	151 (32)	−7 (25)	−48 (25)	54 (26)
	104 (21)	144 (23)	130 (23)	20 (20)	24 (18)	37 (20)
C(9)	30 (8)	66 (9)	96 (11)	3 (7)	14 (8)	18 (9)
	106 (30)	65 (28)	207 (33)	23 (24)	−69 (26)	24 (25)
	66 (20)	110 (23)	204 (25)	25 (19)	−6 (18)	24 (20)

[a] x, y, z are fractional coordinates. The three lines for each atom are the 45, 53, and 60 K parameters in that order. [b] Isotropic temperature factor of the form $\exp(-8\pi^2 U \sin^2\theta/\lambda^2)$. [c] Atoms refined anisotropically. [d] The 53 and 60 K hydrogen temperature factors were not refined. [e] Anisotropic temperature factors of the form $\exp[-2\pi^2(a^{*2}U_{11}h^2 + \ldots + 2a^*b^*U_{12}hk + \ldots)]$.

Table IV. Principal Intramolecular Distances and Angles for (TTF)(TCNQ)

	Distance, Å		
Atoms[a]	60 K	53 K	45 K
S(1)–C(3)	1.738 (4)	1.753 (7)	1.742 (2)
S(2)–C(3)	1.741 (4)	1.739 (6)	1.742 (2)
S(1)–C(1)	1.729 (5)	1.736 (6)	1.732 (2)
S(2)–C(2)	1.731 (5)	1.729 (7)	1.732 (2)
C(3)–C(3)'	1.348 (8)	1.342 (12)	1.369 (4)
C(1)–C(2)	1.314 (6)	1.311 (9)	1.347 (2)
C(1)–H(1)	0.97 (4)	0.78 (6)	0.98 (2)
C(2)–H(2)	0.88 (4)	0.94 (6)	1.02 (2)
C(4)–N(1)	1.144 (6)	1.151 (8)	1.149 (2)
C(5)–N(2)	1.138 (5)	1.143 (7)	1.158 (3)
C(4)–C(6)	1.431 (6)	1.429 (9)	1.434 (2)
C(5)–C(6)	1.428 (6)	1.429 (8)	1.423 (3)
C(6)–C(7)	1.383 (6)	1.395 (8)	1.394 (3)
C(7)–C(8)	1.438 (6)	1.435 (8)	1.443 (3)
C(7)–C(9)	1.435 (6)	1.428 (9)	1.441 (2)
C(8)–C(9)'	1.344 (7)	1.353 (8)	1.344 (3)
C(8)–H(8)	0.89 (4)	1.08 (6)	0.93 (2)
C(9)–H(9)	0.87 (4)	1.01 (8)	0.90 (2)
		Angles, deg	
S(1)–C(3)–C(3)'	122.7 (4)	121.8 (6)	122.2 (2)
S(2)–C(3)–C(3)'	122.8 (4)	123.9 (7)	122.6 (2)
S(1)–C(3)–S(2)	114.5 (2)	114.4 (3)	115.1 (1)
C(3)–S(2)–C(2)	95.0 (2)	95.1 (3)	95.2 (1)
S(2)–C(2)–C(1)	117.7 (4)	117.9 (5)	117.0 (2)
S(1)–C(1)–C(2)	117.8 (4)	117.9 (5)	117.8 (2)
C(1)–S(1)–C(3)	95.0 (2)	94.6 (3)	94.8 (1)
C(7)–C(8)–C(9)'	121.8 (4)	121.0 (6)	121.6 (2)
C(8)–C(7)–C(9)	115.9 (4)	116.3 (5)	116.7 (2)
C(7)–C(9)–C(8)'	122.3 (4)	122.6 (6)	121.8 (2)
C(6)–C(7)–C(8)	122.5 (4)	122.2 (6)	121.7 (2)
C(6)–C(7)–C(9)	121.6 (4)	121.4 (5)	121.6 (2)
C(4)–C(6)–C(7)	120.3 (4)	119.9 (5)	120.8 (2)
C(5)–C(6)–C(7)	121.6 (4)	120.6 (6)	121.1 (1)
C(4)–C(6)–C(5)	118.0 (4)	119.5 (5)	118.1 (2)
C(6)–C(4)–N(1)	177.4 (5)	177.0 (7)	176.9 (2)
C(6)–C(5)–N(2)	176.5 (6)	177.8 (9)	176.5 (2)

[a] The primes associated with TTF atoms indicate their coordinates are transformed by $\bar{x}, \bar{y}, \bar{z}$. For TCNQ atoms, the transformation is $1-\bar{x}, \bar{y}, \bar{z}$.

tances and angles and, in Table V, the least-squares planes and the distances of the atoms from their respective planes are given for each temperature.

The packing of the molecules is summarized in Table VI for the range of temperatures studied. It should be noted that recent evidence has been obtained from diffuse x-ray

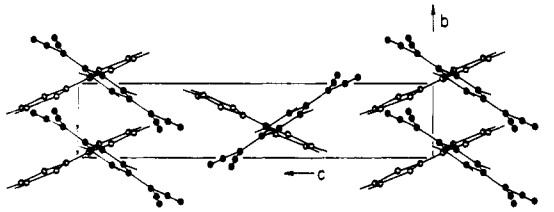

Figure 2. Crystal structure of TTF–TCNQ.

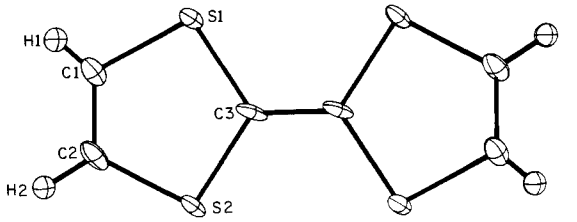

Figure 3. Thermal ellipsoids and labeling scheme for TTF in TTF–TCNQ at 53 K.

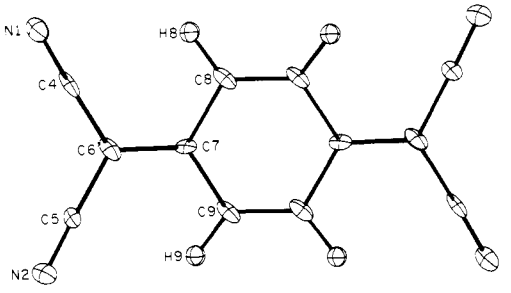

Figure 4. Thermal ellipsoids and labeling scheme for TCNQ in TTF–TCNQ at 53 K.

scattering for a Peierls transition in TTF-TCNQ.[13] However, in our experiments, no superlattice Bragg peaks were observed down to 45 K and the molecules were considered to be equally spaced along the b-axis direction at all temperatures. The decrease in the interplanar distances between room temperature and 45 K is 0.078 (2) Å for TCNQ and 0.064 (2) Å for TTF. In the case of TCNQ, the decrease is due entirely to the contraction of the b axis, while, for TTF, the angle of the molecular plane with the b axis changes slightly (0.7°) resulting in a slightly smaller decrease in the interplanar distance. In addition, the relative orientation of the molecules remains fixed as shown by the angles of the planes with the a and c^* axes. The results

Table V. Least-Squares Planes and the Distances (Å) of the Atoms from Their Respective Planes[a]

In each of the equations of the planes, X, Y, and Z are coordinates (Å) referred to the unit orthogonal axes along a, b, and c^*. The plane equations have the form $AX + BY + CZ = D$ and the coefficients given below are $\times 10^4$.

(a) TTF molecular plane (non-hydrogen atoms)

T (°K)	A	B	C	D
60	172	−9132	−4070	0
53	186	−9134	−4066	0
45	176	−9140	−4053	0

	295 K	100 K	60 K	53 K	45 K
S(1)	0.023 (1)	0.0258 (7)	0.025 (1)	0.022 (2)	0.0264 (4)
S(2)	0.021 (1)	0.0242 (7)	0.024 (1)	0.027 (2)	0.0257 (4)
C(1)	0.008 (3)	−0.016 (3)	−0.015 (5)	−0.008 (7)	−0.016 (2)
C(2)	−0.015 (3)	−0.012 (3)	−0.013 (5)	−0.020 (7)	−0.014 (2)
C(3)	−0.010 (3)	0.013 (3)	0.012 (4)	0.012 (6)	0.014 (2)

(b) TTF central plane defined by S(1), C(3), S(2), and their centrosymmetric mates

T (°K)	A	B	C	D
60	180	−9068	−4212	0
53	172	−9071	−4206	0
45	183	−9072	−4202	0

	295 K	100 K	60 K	53 K	45 K
S(1)	−0.0002 (7)	−0.0004 (7)	0.000 (1)	0.000 (1)	−0.006 (4)
S(2)	−0.002 (7)	−0.004 (7)	0.000 (1)	0.000 (1)	−0.006 (6)
C(1)	−0.058 (3)	−0.066 (3)	−0.065 (5)	−0.055 (7)	−0.068 (2)
C(2)	−0.053 (3)	−0.062 (3)	−0.062 (5)	−0.069 (7)	−0.066 (2)
C(3)	0.001 (3)	0.002 (3)	0.002 (4)	0.001 (6)	0.003 (2)

(c) TCNQ molecular plane (non-hydrogen atoms)

T (°K)	A	B	C	D
60	−183	8280	−5604	−1111
53	−209	8285	−5595	−1277
45	−192	8287	−5593	−1170

	295 K	100 K	60 K	53 K	45 K
N(1)	0.022 (3)	0.018 (2)	0.019 (4)	0.025 (5)	0.018 (2)
N(2)	0.028 (3)	0.029 (2)	0.028 (4)	0.027 (5)	0.028 (2)
C(4)	−0.016 (3)	−0.012 (2)	−0.010 (5)	−0.022 (6)	−0.013 (2)
C(5)	−0.012 (3)	−0.015 (2)	−0.014 (5)	−0.011 (6)	−0.015 (2)
C(6)	−0.024 (3)	−0.022 (2)	−0.024 (4)	−0.019 (6)	−0.019 (2)
C(7)	−0.016 (3)	−0.022 (2)	−0.020 (4)	−0.027 (6)	−0.022 (2)
C(8)	0.000 (3)	0.004 (2)	−0.004 (5)	0.003 (6)	0.005 (2)
C(9)	−0.015 (3)	−0.012 (2)	−0.016 (5)	−0.012 (6)	−0.012 (2)

(d) TCNQ quininoid ring defined by C(6), C(7), C(8), C(9), and their centrosymmetric mates

T (°K)	A	B	C	D
60	−136	8337	−5221	−825
53	−151	8337	−5521	−920
45	−125	8335	−5524	−762

	295 K	100 K	60 K	53 K	45 K
N(1)	0.046 (3)	0.041 (2)	0.050 (4)	0.049 (5)	0.037 (2)
N(2)	0.080 (3)	0.081 (2)	0.080 (4)	0.078 (5)	0.077 (2)
C(4)	0.010 (3)	0.013 (2)	0.020 (5)	0.003 (6)	0.008 (2)
C(5)	0.029 (3)	0.026 (2)	0.028 (5)	0.028 (6)	0.023 (2)
C(6)	0.002 (3)	0.004 (2)	0.004 (4)	0.006 (6)	0.004 (2)
C(7)	−0.002 (3)	−0.009 (2)	−0.005 (4)	−0.014 (6)	−0.010 (2)
C(8)	−0.002 (3)	0.003 (2)	−0.003 (5)	0.002 (6)	0.002 (2)
C(9)	−0.002 (3)	0.003 (2)	−0.003 (5)	0.002 (6)	0.002 (2)

[a] The 295 and 100 K distances are from ref 6 and 7, respectively.

indicate that the very close TCNQ-TCNQ distance of 3.091 (2) Å is reached near the transition and remains relatively constant down to 45 K.

The variation of the lattice constants with temperature (Figure 1) is anomalous for the a and c axes and for the angle β at the transition temperature. Similar behavior has been observed in a single-crystal x-ray diffraction study of TTF-(2,5-diethyl)TCNQ, which undergoes a metal to insulator transition at 110 K.[14] Even though these changes are on the order of the standard deviations, the two independent experiments indicate that there is some type of lattice distortion associated with the transition. In addition, it is observed in TTF-TCNQ that all three axes contract as the temperature is lowered to ~60 K, but remain constant below the transition. This is in agreement with the intermolecular distances calculated from the single-crystal data and indicates that the 54 K transition occurs near the temperature of closest intermolecular approach upon cooling. However, this is not the case in TTF-Et_2TCNQ, for which the cell parameters continue to contract at temperatures below the transition.[14]

A comparison of the intramolecular dimensions at the various temperatures is shown in Tables VII and VIII, where *mmm* symmetry has been assumed for each molecule. The low temperature bond distances have been corrected for rigid body motion by the method of Schomaker and Trueblood,[15] though corrections are all less than one standard deviation. Anisotropic thermal parameters for the carbon and nitrogen atoms are not available for the room temperature structure,[6] and therefore the TCNQ distances are not corrected and the TTF correction is based only on the thermal ellipsoids of the sulfur atoms. It is seen that except for the olefinic bonds in TTF, all changes of bond distances and angles are within approximately two standard deviations. In TTF, the bonds labeled a and d are shortest at 53 K and longest at 45 K, with changes equal to about 2σ

Table VI. Intermolecular Distances and Angular Orientations of the Molecular Planes

	295 K[a]	100 K[b]	60 K	53 K	45 K
TTF–TTF distance (Å)	3.473 (2)	3.426 (1)	3.409 (2)	3.408 (2)	3.409 (1)
TCNQ–TCNQ distance (Å)	3.168 (2)	3.113 (1)	3.091 (2)	3.091 (2)	3.090 (1)
Angle of the normal to the TTF plane with the					
a axis (deg)	89.0	89.0	89.0	88.9	89.0
b axis (deg)	24.6	24.1	24.0	24.0	23.9
*c** axis (deg)	65.4	65.9	66.0	66.0	66.1
Angle of the normal to the TCNQ plane with the					
a axis (deg)	89.0	89.0	89.0	88.8	88.9
b axis (deg)	34.0	34.0	34.1	34.1	34.0
*c** axis (deg)	56.1	56.0	55.9	56.0	56.0

[a] Reference 6. [b] Reference 7.

Table VII. Dimensions of TTF Molecules Averaged over Assumed *mmm* Symmetry[a]

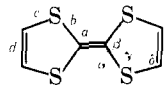

	TTF–TCNQ					TTF[0]
	295 K[b]	100 K[c]	60 K	53 K	45 K	295 K[d]
a (Å)	1.372 (4)	1.366 (5)	1.349 (8)	1.343 (12)	1.370 (4)	1.349 (3)
b	1.745 (3)	1.745 (2)	1.741 (3)	1.749 (5)	1.743 (2)	1.757 (2)
c	1.739 (3)	1.736 (2)	1.731 (4)	1.734 (5)	1.733 (2)	1.726 (2)
d	1.326 (4)	1.336 (3)	1.315 (6)	1.313 (9)	1.349 (2)	1.314 (3)
α (deg)	122.6 (2)	122.5 (2)	122.8 (3)	122.9 (5)	122.4 (2)	122.8 (1)
β	114.7 (3)	144.9 (1)	114.5 (2)	114.4 (2)	115.1 (1)	114.5 (2)
γ	95.0 (2)	95.0 (1)	95.0 (1)	94.9 (2)	95.0 (1)	94.4 (1)
δ	117.4 (1)	117.5 (2)	117.8 (3)	117.9 (4)	117.4 (2)	118.3 (1)

[a] The 100–45 K distances in TTF–TCNQ have been corrected for rigid-body motion. The 295 K distances are partially corrected (see text). The TTF[0] distances are uncorrected. [b] Reference 6. [c] Reference 7. [d] Reference 16.

Table VIII. Dimensions of TCNQ Molecules Averaged over Assumed *mmm* Symmetry[a]

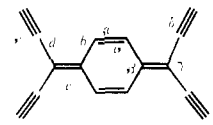

	TTF–TCNQ					TCNQ[0]	TCNQ[−]
	295 K[b]	100 K[c]	60 K	53 K	45 K	295 K[d]	113 K[e]
a (Å)	1.356 (3)	1.352 (4)	1.345 (7)	1.353 (4)	1.343 (3)	1.346 (3)	1.373 (4)
b	1.433 (3)	1.435 (3)	1.437 (4)	1.431 (6)	1.444 (3)	1.448 (4)	1.423 (4)
c	1.402 (3)	1.395 (3)	1.383 (6)	1.396 (8)	1.393 (3)	1.374 (3)	1.420 (4)
d	1.423 (3)	1.434 (3)	1.431 (4)	1.429 (6)	1.430 (3)	1.440 (4)	1.416 (4)
e	1.151 (4)	1.150 (3)	1.142 (4)	1.148 (5)	1.155 (3)	1.140 (3)	1.153 (4)
α (°)	121.4 (2)	121.5 (2)	122.0 (3)	121.8 (4)	121.7 (2)	121.0 (2)	121.0 (3)
β	117.2 (2)	116.9 (2)	115.9 (4)	116.3 (5)	116.7 (2)	118.1 (2)	118.0 (3)
γ	117.8 (2)	118.0 (2)	118.0 (4)	119.5 (5)	118.1 (2)	115.9 (2)	116.3 (3)
δ	177.1 (2)	177.0 (2)	177.4 (4)	177.4 (6)	117.6 (2)	179.5 (2)	179.2 (3)

[a] All distances except 295 K TTF–TCNQ and $TCNQ^-$ are corrected for rigid body motion. [b] Reference 6. [c] Reference 7. [d] R. E. Long, R. A. Sparks, and K. N. Trueblood, *Acta Crystallogr.*, 18, 932 (1965). [e] A. Hoekstra, T. Spoelder, and A. Vos, *Acta Crystallogr., Sect. B,* 28, 14 (1972).

and 4σ, respectively. Furthermore, the distances at 53 K of 1.343 (12) and 1.313 (9) Å approach the neutral TTF room temperature distances of 1.349 (3) and 1.314 (3) Å[16] for *a* and *d*, respectively.

It must be emphasized that the differences in the bond distances are in all cases less than 4σ. However, though it is possible there are other factors responsible for these observations, such as anharmonic vibrational modes, the changes are systematic and are consistent with a model in which the degree of charge transfer between TTF and TCNQ decreases as the conductivity increases. At 45 K, the complex is in an insulating state and the *a* and *d* bonds are equal to or longer than their respective distances at room temperature. The only anomaly in the decrease of the olefinic bonds from 295 to 53 K is in bond distance *d*, which appears to be shorter at room temperature than at 100 K. However, thermal libration of the molecule should be greatest at room temperature, but these distances could be only partially corrected (*vide ante*).

In TCNQ, molecular orbital calculations indicate[17] that bonds *a* and *c* should be the most sensitive to molecular charge. The systematic changes for these bonds shown in Table VIII are generally compatible with those of TTF if they are due to changes in the degree of charge transfer.

Table IX. Rigid-Body Thermal Parameters[a]

(a) TTF — Axes in the system of inertia

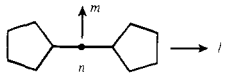

L Tensor Elements × 10^4 rad²

T (°K)	L_{11}	L_{12}	L_{13}	L_{22}	L_{23}	L_{33}
100	38 (7)	−1 (1)	−2 (3)	5 (2)	0 (1)	9 (1)
60	11 (9)	2 (2)	−3 (3)	2 (2)	−2 (2)	12 (2)
53	7 (15)	1 (3)	−5 (6)	4 (3)	−3 (3)	10 (3)
45	10 (8)	−1 (2)	0 (3)	1 (2)	−1 (2)	4 (2)

T Tensor Elements × 10^4 Å²

T (°K)	T_{11}	T_{12}	T_{13}	T_{22}	T_{23}	T_{33}
100	148 (6)	0 (6)	5 (6)	92 (9)	−4 (9)	103 (14)
60	133 (8)	17 (7)	13 (8)	60 (11)	1 (11)	128 (17)
53	165 (13)	70 (13)	36 (14)	90 (19)	34 (19)	115 (30)
45	70 (7)	−5 (7)	2 (8)	40 (10)	−7 (10)	68 (16)

Principal Axes

	L				*T*			
T (°K)	Rms amplitudes (deg)	Direction cos × 10^4 *l*	*m*	*n*	Rms amplitudes (Å)	Direction cos × 10^4 *l*	*m*	*n*
100	3.5	−9968	292	744	0.12	−9939	−70	1099
	1.7	−697	1388	−9879	0.10	−1065	3176	−9422
	1.3	−392	−9899	−1363	0.10	−283	−9482	−3165
60	2.2	5496	1824	−7830	0.12	−8050	−1617	−5709
	1.7	7925	311	6091	0.11	−5523	−1474	8205
	0.7	1355	−9827	−1261	0.08	−2168	9758	294
53	2.2	−5443	−2962	7849	0.15	−7739	−4927	−3979
	1.2	−7433	6041	−2875	0.10	−4411	−315	8969
	0.8	−3890	−7399	−5489	0.07	−4544	8696	−1930
45	1.8	−9949	949	328	0.09	7552	−2294	6140
	1.2	−110	2213	−9752	0.08	6429	767	−7621
	0.5	−998	−9706	−2191	0.06	1277	9703	2054

(b) TCNQ — Axes in the system of inertia

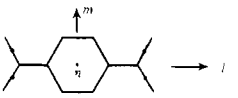

L Tensor Elements × 10^4 rad²

T (°K)	L_{11}	L_{12}	L_{13}	L_{22}	L_{23}	L_{22}
100	31 (1)	0 (1)	0 (2)	2 (2)	−1 (1)	4 (1)
60	14 (6)	−2 (1)	−1 (1)	1 (2)	−1 (1)	2 (1)
53	8 (8)	0 (1)	0 (2)	3 (2)	0 (1)	1 (1)
45	19 (5)	0 (1)	0 (1)	0 (1)	0 (1)	1 (1)

T Tensor Elements × 10^4 Å²

T (°K)	T_{11}	T_{12}	T_{13}	T_{22}	T_{23}	T_{33}
100	133 (8)	−5 (8)	9 (9)	109 (12)	−6 (12)	57 (14)
60	158 (8)	8 (8)	−17 (9)	119 (12)	−37 (12)	80 (14)
53	171 (10)	62 (10)	−41 (10)	153 (14)	−57 (14)	65 (17)
45	82 (6)	8 (6)	−2 (6)	65 (9)	−1 (1)	24 (10)

Principal Axes

	L				*T*			
T (°K)	Rms amplitudes (deg)	Direction cos × 10^4 *l*	*m*	*n*	Rms amplitudes (Å)	Direction cos × 10^4 *l*	*m*	*n*
100	3.2	10000	−92	. 33	0.12	−9687	2118	−1295
	1.2	55	2452	−9695	0.10	−2217	−9728	672
	0.8	81	9694	2452	0.07	−1118	938	9893
60	2.2	−9884	1136	1009	0.13	−8585	−3899	3331
	0.9	−304	5025	−8640	0.11	−5012	7759	−3832
	0.4	−1488	−8571	−4933	0.08	−1091	−4959	−8615
53	1.6	−9969	−710	352	0.16	−6852	−6392	3492
	0.9	−614	9730	2227	0.10	−7216	6610	−2060
	0.5	−501	2198	−9742	0.06	−991	−3931	−9141
45	2.5	−9999	114	88	0.09	−9354	−3525	275
	0.7	−88	−181	−9998	0.08	−3526	9358	3
	0.2	−114	−9998	181	0.05	−258	−94	−9996

[a] All tensor and direction cosines are referred to the inertial system.

However, there are 16 bonds in TCNQ vs. only 10 in TTF, so that the bond lengths in TCNQ should be less sensitive to changes in molecular charge. This appears to be the case.

Since a closer interplanar distance results in greater intermolecular orbital overlap, it is worthwhile to examine charge transfer vs. TCNQ interplanar distance. An analogy can be made with the partially oxidized tetracyanoplatinate complexes, where it is seen that, in general, slightly greater oxidation results in a shorter Pt-Pt distance.[18] For example, the complexes with Pt oxidation numbers of +2.32 and +2.30 have Pt-Pt distances of 2.88 and 2.89 Å, respectively, while the complexes with oxidation numbers of +2.28 and +2.26 have Pt-Pt distances of 2.99 and 2.96 Å, respectively. In addition, Interrante and Bundy[19] have shown that the conductivity of $K_2Pt(CN)_4Br_{0.3}\cdot 2.3H_2O$ increases with increasing pressure up to ~35 kbar, which corresponds to a decrease of ~0.07 Å in the Pt-Pt distance. These properties have been explained in terms of the decreasing metal-metal distance resulting in greater orbital overlap and higher conductivity.[19] Bloch and Weisman[20] suggest that a decreasing lattice repeat distance should result in fewer electrons in a one-dimensional conduction band. If one considers less charge transfer as oxidation of $TCNQ^-$ and reduction of TTF^+, the same type of band description could apply to TTF-TCNQ above the transition temperature. It is possible that the unusual properties of TTF-TCNQ are related to changes in oxidation states with decreasing intermolecular distances *in the crystalline state*. In the tetracyanoplatinate salts, the oxidation state of the platinum is established during crystallization by the stoichiometry and this does not change with temperature.

Though a comparison of the bond lengths in TTF-TCNQ with those in neutral TCNQ and its various salts gives some indication of the amount of charge transfer between the component molecules, the result depends on the assumption that in salts as NaTCNQ a full electron has been transferred. When accurate x-ray data are available, direct evaluation of the charge transfer can be made by integration of the observed electron density over the molecular volume. If the molecular volume can be enclosed by a parallelpiped or some other well-defined body, the integration may be performed analytically.[21] Application of this technique to the pyrene tetracyanoethylene complex has shown the charge transfer in the ground state of the complex to be zero.[22] The technique was applicable in this case because of the regular (almost square) shape of the TCNE molecule. For TTF-TCNQ, however, a number of attempts to describe the molecular volumes by an easy to integrate *analytical* expression failed, as invariably parts of adjacent molecules were included.

A *numerical* integration technique was therefore developed which is of much more general applicability, and which will be described in full detail elsewhere.[23] Briefly, the method consists of a subdivision of the unit cell volume into small parallelpipeds (typically 0.25 × 0.25 × 0.25 Å). The density is integrated over each of the parallelpipeds separately and subsequently summed over the molecular volume. The subvolumes in the intermolecular region are

assigned to either of the adjacent molecules on the basis of the ratio of the van der Waals radii of the atoms in its proximity. If r_A is the distance to atom A with radius R_A and r_b the distance to atom B with radius R_B, the subvolume is assigned to the molecule containing the atom with the smallest value of the ratio r_i/R_i. This procedure leads to a complete assignment of all space in the crystal and is applicable to any molecular shape. Errors are evaluated as described by Coppens and Hamilton,[21] using an approximate single volume element for the molecule.

The results of the calculation are mildly dependent on the choice of van der Waals radii. Using a set given by Pauling (S, 1.85; C, 1.85; N, 1.5; H, 1.1 Å) a value of 0.45 ± 0.15 electron is obtained for the transfer from TTF to TCNQ at 100 K. A different choice of radii (S, 1.85; C, 1.65; N, 1.55; H, 1.2 Å) leads to increased transfer, due to the increase in some of the peripheral atoms of the TCNQ componet molecule. Nevertheless, the result of 0.50 ± 0.15 electron is not significantly different from that obtained earlier. The results can by summarized as providing definite evidence for transfer of electrons from TTF to TCNQ and as being compatible with an average transfer of less than an electron. With more accurate diffraction data, it should be possible to reduce the standard deviation in the result, which may make a study of the temperature dependence of the integrated charge feasible. Such an extension is presently being considered.

In Table V, the distances of the atoms from the least-squares mean planes are tabulated. It is seen that in both TTF and TCNQ, the terminal atoms deviate from the central planes so that both molecules have a chair conformation. The deviations from the planes remain essentially constant throughout the temperature range, but it has been noted previously[6] that molecular charge does not appear to affect the planarity of the molecules.

It was originally proposed[2b] that enhancement of electron-phonon interactions at the transition temperature results in the "superconducting" fluctuations. Since the Debye-Waller factor for the elastic scattering of x-radiation is approximately inversely proportional to the frequency of the atomic oscillations,[24] it might be possible to find evidence for a soft phonon mode (a lattice vibration with a frequency approaching zero) by examination of the rigid-body thermal parameters. Morawitz[25] has recently proposed an orientational Peierls transition for TTF-TCNQ for which a rotational displacement of ~1° in the librational motion about axis l of the TCNQ molecule was calculated. This corresponds to a change of 0.9° between the 53 and 45 K structures. As seen in other structural studies,[15] the largest principal axis of libration for TCNQ coincides with the inertial axis l shown in the figure in Table IX. In addition, the root mean square amplitudes are small, as would be expected, in comparison to molecules at room temperature. However, for the TCNQ molecule, it is seen that from 100 to 53 K there is a decrease in the librational amplitudes, but in going from 53 to 45 K the amplitudes increase. Correspondingly, the translational root mean square amplitudes appear to increase slightly from 100 to 53 K, but the 45 K values are seen to be smaller than those at 100 K. Furthermore, the principle axes for both L and T have very similar orientations with respect to the inertial system at 100 and 45 K, but differ significantly at the in-between temperatures. Regardless of whether or not these observations indicate the existence of a soft phonon mode, there does appear to be systematic changes in the thermal parameters associated with the transition at 53 K.

In conclusion, the upper limits have been established for any transition based on a lattice distortion associated with the 53 K transition. We do see evidence for unusual changes in the lattice constants near the transition temperature. However, with respect to the techniques which we have used, there is no observable static lattice transition associated with a change in symmetry or cell doubling to 45 K. Other properties of the crystalline complex that do appear to be related to the metal-insulator transition temperature are small, but systematic, changes in the intramolecular bond distances and rigid-body thermal parameters.

Acknowledgment. The support of the National Science Foundation under Grants NSF-DMR-7203026 and MPS-71-02783 is gratefully acknowledged.

Supplementary Material Available: structure factor amplitudes (25 pages). Ordering information is given on any current masthead page.

References and Notes

(1) (a) University of Illinois; (b) State University of New York at Buffalo.
(2) (a) J. Ferraris, D. O. Cowan, V. Walatea, and J. Perlstein, *J. Am. Chem. Soc.*, **95**, 948 (1973); (b) L. B. Coleman, N. J. Cohen, D. J. Sandman, F. G. Yamagishi, A. F. Garito, and A. J. Heeger, *Solid State Commun.*, **12**, 1125 (1973).
(3) R. P. Groff, A. Sunce, and R. E. Merrefield, *Phys. Rev. Lett.*, **33**, 418 (1974).
(4) B. Renker, H. Rietschel, L. Pintschovious, W. Gläser, P. Brüesch, D. Kuse, and M. J. Rice, *Phys. Rev. Lett.*, **30**, 1144 (1973).
(5) R. Comes, M. Lambert, H. Leounois, and H. R. Zeller, *Phys. Rev. B.*, **8**, 571 (1973).
(6) T. J. Kistenmacher, T. E. Phillips, and D. O. Cowan, *Acta Crystallogr., Sect. B*, **30**, 763 (1974).
(7) R. H. Blessing and P. Coppens, *Solid State Commun.*, **15**, 215 (1974).
(8) R. A. Craven, M. B. Salamon, G. DePasquali, R. M. Herman, G. Stucky, and A. Schultz, *Phys. Rev. Lett.*, **32**, 769 (1974).
(9) (a) S. Etemad, T. Penney, and E. M. Engler, *Bull. Am. Phys. Soc.*, **20**, 496 (1975); S. Etemad, to be submitted for publication; (b) M. B. Salamon, J. W. Bray, G. DePasquali, R. A. Craven, G. Stucky, and A. Schultz, *Phys., Rev. B*, **11**, 619 (1975).
(10) P. Coppens, F. K. Ross, R. H. Blessing, W. F. Cooper, F. K. Larsen, J. G. Leipoldt, B. Rees, and R. Leonard, *J. Appl. Crystallogr.*, **7**, 315 (1974).
(11) The powder data were measured by G. A. Jones, Central Research Department, du Pont (private communication from L. J. Guggenberger).
(12) See paragraph at end of paper regarding supplementary material.
(13) (a) F. Denoyer, F. Comés, A. F. Garito, and A. J. Heeger, *Phys. Rev. Lett.*, **35**, 445 (1975); (b) S. Kagoshima, H. Anzai, K. Kajimura, and T. Ishiguro, *J. Phys. Soc. Jpn.*, in press.
(14) A. J. Schultz and G. D. Stucky, submitted for publication.
(15) V. Schomaker and K. N. Trueblood, *Acta Crystallogr., Sect. B*, **24**, 63 (1968).
(16) W. F. Cooper, N. C. Kenney, J. W. Edmonds, A. Nagel, F. Wudl, and P. Coppens, *Chem. Commun.*, 889 (1971); W. F. Cooper, J. W. Edmonds, F. Wudl, and P. Coppens, *Cryst. Struct. Commun.*, **3**, 23 (1974).
(17) H. Johansen, *Int. J. Quantum Chem.*, **9**, 459 (1975).
(18) K. Krogmann, *Angew. Chem., Int. Ed. Engl.*, **8**, 35 (1969). In this reference, Krogmann states: "There appears to be no strict relationship between Pt–Pt distance and the oxidation number." This is true when considering all of the partially oxidized platinum complexes, but, among the tetracyanoplatinates, there does appear to be a general trend such that higher oxidation results in a smaller Pt–Pt distance.
(19) L. V. Interrante and F. P. Bundy, *Solid State Commun.*, **11**, 1641 (1972).
(20) A. N. Bloch and R. B. Weisman, "Extended Interactions between Metal Ions in Transition Metal Complexes," L. V. Interrante, Ed., ACS Symposium Series 5, Washington, D.C., 1974, p 356.
(21) P. Coppens and W. C. Hamilton, *Acta Crystallogr., Sect. B*, **24**, 925 (1968).
(22) F. K. Larsen, R. G. Little, and P. Coppens, *Acta Crystallogr., Sect. B*, **31**, 430 (1975).
(23) P. Coppens, *Phys. Rev. Lett.*, **35**, 98 (1975), and to be submitted.
(24) C. Kittel, "Introduction to Solid State Physics", 4th ed, Wiley, New York, N.Y., 1971, p 85.
(25) H. Morawitz, *Phys. Rev. Lett.*, **34**, 1096 (1975).